Chemical Engineering Journal 474 (2023) 145548

Contents lists available at ScienceDirect

Chemical Engineering Journal

journal homepage: www.elsevier.com/locate/cej

Active kinetic chain length: Guide for control in atom transfer radical polymerization

Jing Lyu [a,b], Yinghao Li [a], Zishan Li [a], Melissa Johnson [a], Stanislaw Sosnowski [c], Ryszard Szymanski [c,*], Krzysztof Matyjaszewski [d,*], Wenxin Wang [a,b,*]

[a] Charles Institute of Dermatology, School of Medicine, University College Dublin, Dublin 4, Ireland
[b] School of Mechanical and Materials Engineering, University College Dublin, Dublin 4, Ireland
[c] Centre of Molecular and Macromolecular Studies, Polish Academy of Sciences, Sienkiewicza 112, Lodz 90-363, Poland
[d] Center for Macromolecular Engineering, Department of Chemistry, Carnegie Mellon University, Pittsburgh, PA 15213, USA

ARTICLE INFO

Keywords:
ATRP
Active Kinetic Chain Length
Fraction of terminated chains
Dispersity
Monte Carlo simulation

ABSTRACT

Since atom transfer radical polymerization (ATRP) was developed, various strategies have been adopted to design well-controlled ATRP procedures. However, there is no single criterion that could be used for various ATRP reaction conditions (e.g., different monomers, different targeted degrees of polymerization, conversions, etc.). In this work, we introduce a new factor - Active Kinetic Chain Length (AKCL) as a parameter that can guide the design of well-controlled ATRPs. Under a certain reaction system with a specific monomer type (k_p), monomer concentration ($[M]_0$), and targeted degrees of polymerization, the smaller value of AKCL, i.e., a smaller initial number of monomer units added to a growing chain during a chain active period, can decrease polymer dispersity and also diminish the radical termination. The effects of AKCL were compared with other parameters affecting dispersity and livingness in ATRPs, which clearly demonstrates the design principle of AKCL. The model examples of deactivation-enhanced ATRP (DE-ATRP) have further shown the effectiveness of this criterion.

1. Introduction

The radical polymerization of vinyl monomers is one of the most widely used chemical processes to produce synthetic polymers. The conventional free radical polymerization (FRP) of vinyl monomers has been employed to prepare many commercial products.[1-3] In a FRP system, radicals are continuously generated, and in the meantime rapidly die,[3-6] thus, the produced polymers cannot have a well-controlled molecular weight (MW) and narrow molecular weight distribution (MWD, i.e., low dispersity, $Đ$). Moreover, the life of growing chains is too short to perform any synthetic manipulation. To achieve a precise macromolecular design and synthesis, controlled/living radical polymerization, recently termed reversible deactivation radical polymerizations (RDRPs)[7-9], have been developed during the past two decades, including atom transfer radical polymerization (ATRP),[10-12] reversible addition-fragmentation chain-transfer (RAFT) polymerization,[13] and nitroxide-mediated radical polymerization (NMP).[14].

ATRP, as one of the most often studied RDRPs, has been commonly used to design and synthesize polymeric materials with well-defined structures and functionalities.[15-17] To achieve good control in the ATRP systems, several design rules/factors have been employed, including choosing highly efficient catalysts and initiators, using semi-batch operations, ensuring low radical concentrations etc. to control the dispersity ($Đ$),[18-21] and reduce the fraction of terminated chains (FTC).[22-26] However, these strategies are typically designed for specific reaction conditions, which cannot be universally extended to all ATRP systems. For example, when the monomer changes from methyl acrylate (MA, with high propagation rate constant, k_p) to styrene (St, low k_p), the original set of reaction parameters (initiator, catalyst structures and concentrations) are no longer effective to achieve good control.[23] Hence, we have been seeking to find a universal factor that could define control in ATRP systems. In this work, analytical equations and Monte Carlo simulations were both employed to compare the effects of adjusting various single parameters on $Đ$ and FTC in ATRP systems. Based on that, we introduce a new factor - Active Kinetic Chain Length (AKCL) as a parameter to guide design of ATRPs and show that the smaller Active Kinetic Chain Length (AKCL, i.e., the lower initial number of monomer units added to a growing chain during an active period) can

* Corresponding authors.
E-mail addresses: ryszard.szymanski@cbmm.lodz.pl (R. Szymanski), km3b@andrew.cmu.edu (K. Matyjaszewski), wenxin.wang@ucd.ie (W. Wang).

https://doi.org/10.1016/j.cej.2023.145548
Received 25 June 2023; Received in revised form 11 August 2023; Accepted 18 August 2023
Available online 22 August 2023

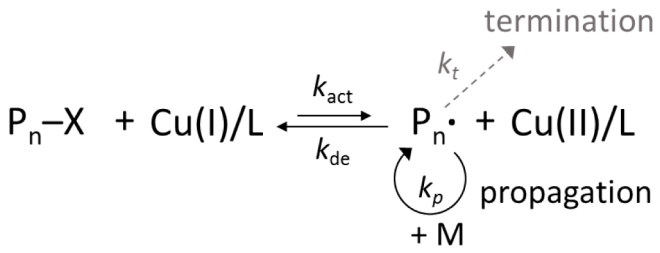

Scheme 1. Schematic illustration of the mechanism of ATRP.

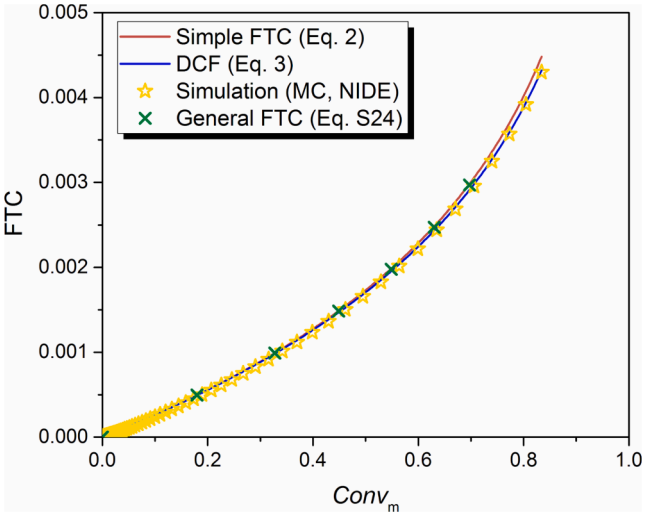

Fig. 1. Relationship between the fraction of terminated chains (FTC) and monomer conversion ($Conv_m$) in ATRP. Results from numerical simulations (Monte Carlo and NIDE) and from analytical equations: DCF - Eq. (3) (with time scale taken from simulations), simple FTC - Eq. (2) and general FTC - Eq. S24. $[M]_0 = 5$ M, $[Ini]_0 = 5x10^{-2}$ M, $[Cu(II)]_0 = 7.5x10^{-3}$ M, and $[Cu(I)]_0 = 5x10^{-3}$ M, T = 25 °C. Reaction rate constants are listed in Table S1.

simultaneously suppress the radical termination and generate polymers with lower dispersity - narrower MWD. AKCL can be used as a general criterion for achieving a well-controlled ATRP process.

2. Results and discussion

2.1. Introduction of the concept of AKCL

The concept of AKCL defined in this work differs from the traditional kinetic chain length term used in polymer chemistry (the rate of chain propagation divided by the sum of the rates of all of chain-termination processes).[27] Herein, AKCL is defined as the initial number of monomer units added to the chain end in its active state, which corresponds to the initial ratio of the propagation rate to the rate of transformation of the active to dormant (deactivated) chain. A similar parameter was previously considered important for ATRP, however, because this parameter varies during polymerization it was termed as the instantaneous kinetic chain length.[28] The equation defining AKCL, is shown in Eq. (1), where the propagation rate is the product of the propagation rate constant k_p, the initial monomer concentration $[M]_0$ and the radical concentration, and the deactivation rate of radicals is the product of the deactivation rate constant k_{de}, the deactivator concentration [Cu(II)] and the radical concentration (this term appears as a factor in both the numerator and denominator of Eq. (1), leading to its cancellation). From Eq. (1), it can be seen that for a particular ATRP system with a defined k_p and $[M]_0$, AKCL depends on the deactivation rate (k_{de}[Cu(II)]). The larger k_{de} and/or the higher concentration of the

Table 1
Effect of various parameters on fraction of terminated chains and polymer dispersity.

	Parameters being analyzed (their effect on AKCL given in parentheses: increase, decrease, no effect)[**]	Influence on FTC[a] (better: decrease of FTC, worse: increase of FTC, or NE: no effect)	Influence on Đ[a] (better: decrease of Đ, worse: increase of Đ, or NE: no effect)
1	All concentrations being changed by dilution, DP_T constant[b] (no effect on AKCL)	NE	NE
2	Only $[M]_0$ being increased, DP_T changes correspondingly (AKCL increases with increasing $[M]_0$)	NE (comparing the same conversion) better (comparing the same DP_n)[c]	better (comparing the same conversion)[c] worse (comparing the same DP_n)[c]
3	Only $[P\text{-}X]_0$ being increased, DP_T changes correspondingly (no effect on AKCL)	better (comparing the same conversion)[d] worse (comparing the same DP_n)[d]	worse (comparing the same conversion)[d] better (comparing the same DP_n)[d]
4	Both $[M]_0$ and $[P\text{-}X]_0$ being increased, DP_T constant (AKCL increases with increasing $[M]_0$)	better[e]	worse[e]
5	Only $Conv_m$ being increased (no effect on AKCL)	worse[f]	better[f]
6	Only $[Cu(I)]_0$ being increased (no effect on AKCL)	worse[g]	NE*
7	Only $[Cu(II)]_0$ being increased (AKCL decreases with increasing $[Cu(II)]_0$)	better[h]	better[h]
8	Only k_{de} being increased (AKCL decreases with increasing k_{de})	better[i]	better[i]
9	Both k_{de} and k_{act} being increased, the ratio k_{act}/k_{de} constant (AKCL decreases with increasing k_{de})	NE	better[j]

[a] According to the equations for DCF/FTC (Eqs. (2) and (3)) and Đ (Eqs. (4) to (6)) and to the Monte Carlo simulations of ATRP of MA (Fig. 2 to Fig. 7, Fig. S1 and S2, Table S2 to S9)

[b] $[M]_0$, $[P\text{-}X]_0$, $[Cu(I)]_0$, and $[Cu(II)]_0$ were changed by diluting the system with solvent while keeping DP_T constant (Table S2, Fig. 2).

[c] Increasing $[M]_0$ by 5 times made Đ *ca.* 1.02–1.1 times lower comparing the same $Conv_m$, and *ca.* 1.02–1.17 times higher comparing the same DP_n; FTC is *ca.* 3–15 times lower comparing the same DP_n (Fig. 3).

[d] Increasing $[P\text{-}X]_0$ by 5 times made Đ *ca.* 1.02–1.17 times higher and FTC *ca.* 1.09–1.67 times lower comparing the same $Conv_m$; Đ and FTC are *ca.* 1.003 times lower and *ca.* 3.4–8.4 times higher comparing the same DP_n (Fig. 4). [e]Increasing both $[M]_0$ and $[P\text{-}X]_0$ by 5 times made Đ *ca.* 1.003–1.12 times higher and FTC *ca.* 1.05–2.25 times lower (Fig. S1).

[f] Increasing $Conv_m$ from 10% to 50% made Đ 1.09 times lower and FTC 5.19 times higher (Fig. 2).

[g] Increasing $[Cu(I)]_0$ by 5 times made FTC *ca.* 2–5.55 times higher (Fig. 5).

[h] Increasing $[Cu(II)]_0$ by 10 times made Đ *ca.* 1.007–1.22 times lower and FTC *ca.* 3–7.42 times lower (Fig. 6).

[i] Increasing k_{de} by 6.67 times made Đ *ca.* 1.01–1.21 times lower and FTC *ca.* 2–10 times lower (Fig. 7).

[j] Increasing both k_{de} and k_{act} by 6.67 times made Đ *ca.* 1.006–1.21 times lower (Fig. S2).

[**] The above magnitures of changes are only for the example ATRP systems in Fig. 2 to Fig. 7, Fig. S1 and S2, which would change when the reference system changes.

[*] There is a slight improvement due to higher [Cu(II)] generated in ATRP systems with low initial [Cu(II)] (Table S14, Fig. S7).

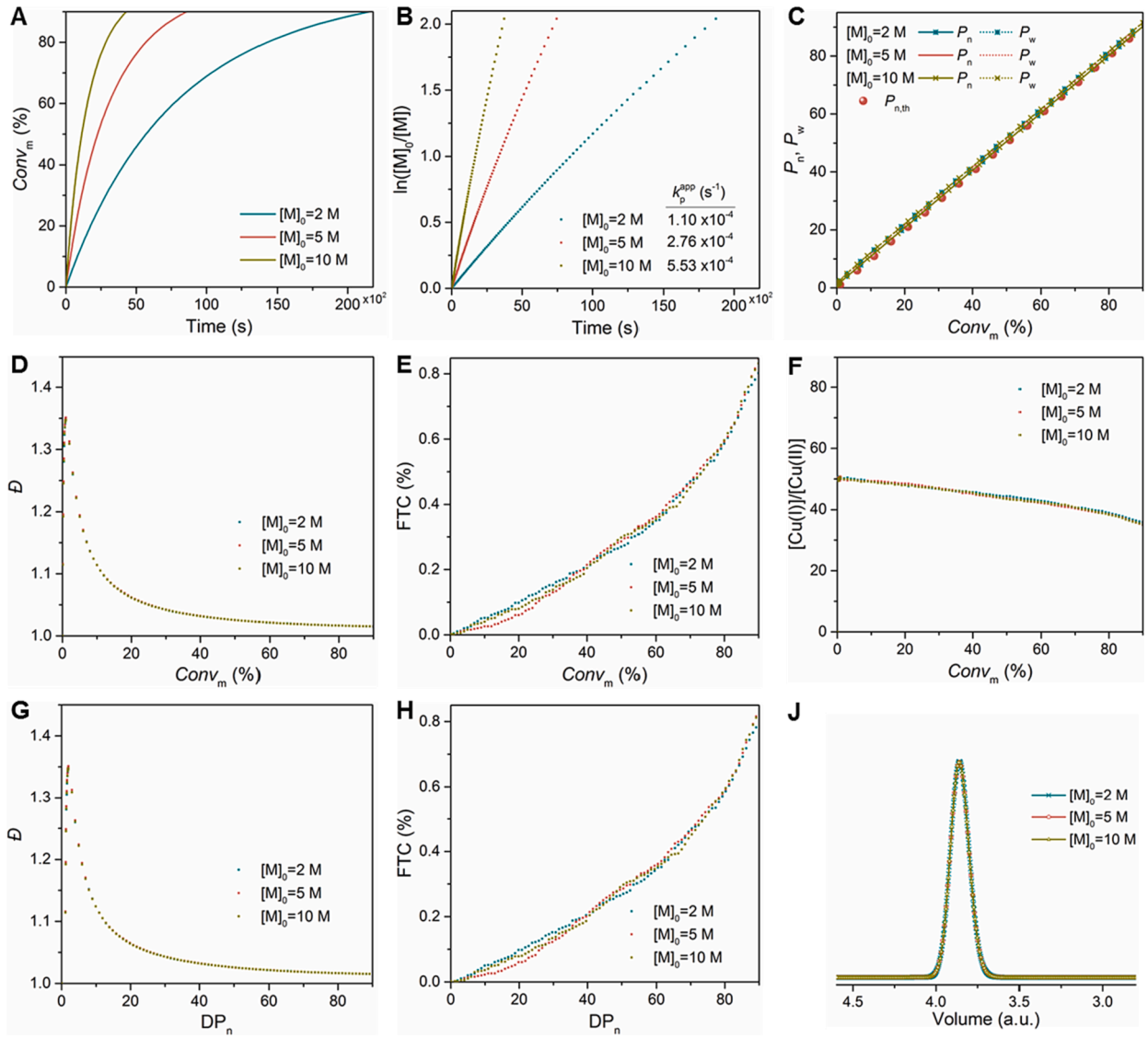

Fig. 2. Monte Carlo simulations of ATRP of MA with different $[M]_0$. Kinetic plots of (**A**) $Conv_m$, (**B**) $\ln([M]_0/[M])$ *versus* time (where k_p^{app} is the pseudo-first-order apparent propagation rate constant, i.e., the slope of the semilogarithmic kinetic plots). We compute k_p^{app} values assuming linearity of $\ln([M]_0/[M])$ *versus* time and thus these quantities are the average ones, similarly as [R·]. Changes of (**C**) P_n, P_w, (**D**) $Đ$, (**E**) FTC, and (**F**) [Cu(I)]/[Cu(II)] with $Conv_m$. Changes of (**G**) $Đ$, and (**H**) FTC with DP_n. (**J**) MWD at $Conv_m = 80\%$. Results were obtained from Monte Carlo simulations of ATRP of MA at 25 °C with $[M]_0 = 2$, 5, and 10 M, $[P\text{-}X]_0 = 0.02$, 0.05, and 0.1 M, $[Cu(I)]_0 = 0.02$, 0.05, and 0.1 M, $[Cu(II)]_0 = 0.0004$, 0.001, and 0.002 M, respectively (no effect on AKCL), $[M]_0/[P\text{-}X]_0$ is 100/1 (Table S2).

deactivator ([Cu(II)]), the smaller the AKCL.

$$AKCL = \frac{\text{Rate(propagation)}}{\text{Rate(deactivation)}} = \frac{k_p[M]_0}{k_{de}[Cu(II)]} \quad (1)$$

2.2. New equation for livingness and reformulation for dispersity in ATRP

To understand the effect of AKCL (i.e., [Cu(II)] and/or k_{de}) on the preservation of chain end functionality, in this work, a new equation to correlate the fraction of terminated chains (FTC) in ATRP systems with conversion was derived by taking the deactivation into account. The possibility of different reactivity of growing radicals in RDRP, in relation to their sizes, interactions or spatial vicinity, was disregarded[29,30]. Thus, the reactivity of all radicals was assumed identical. Eq. (2) was derived by assuming a constant ratio of [Cu(I)]/[Cu(II)]. A general equation (Eq. S24 or Eq. S25) without this restriction was also derived (see detailed derivation process in the Supplementary Information).

$$FTC = \frac{[T]}{[P-X]_0} = 1-(1-Conv_m)^{\frac{k_t \times k_{act}[Cu(I)]}{k_p \times k_{de}[Cu(II)]}} = 1-(1-Conv_m)^{AKCL \times \frac{k_t \times k_{act}[Cu(I)]}{k_p^2 \times [M]_0}} \quad (2)$$

where [T] is the concentration of terminated chains (not the concentration of dead chains), $[P\text{-}X]_0$ is the initial concentration of initiators (i.e., $[Ini]_0$). [Cu(I)], [Cu(II)], $Conv_m$, k_p, k_t, k_{de}, and k_{act} are the activator concentration, deactivator concentration, monomer conversion, rate constant of propagation, termination, deactivation and activation, respectively (Scheme 1).

Eq. (2) is somehow different from Eq. (3) – dead chain fraction (DCF). From the definition aspect, DCF calculates the fraction of dead chains, while FTC calculates the fraction of terminated chains. Therefore, if the termination in an ATRP system proceeds mainly *via* the combination of radicals, the value of DCF (the number of dead chains) should be twice lower than the FTC (the number of terminated ones). But for small FTC (below a few %),[31] they give essentially the same predicted values of terminated chains, the deviation became more

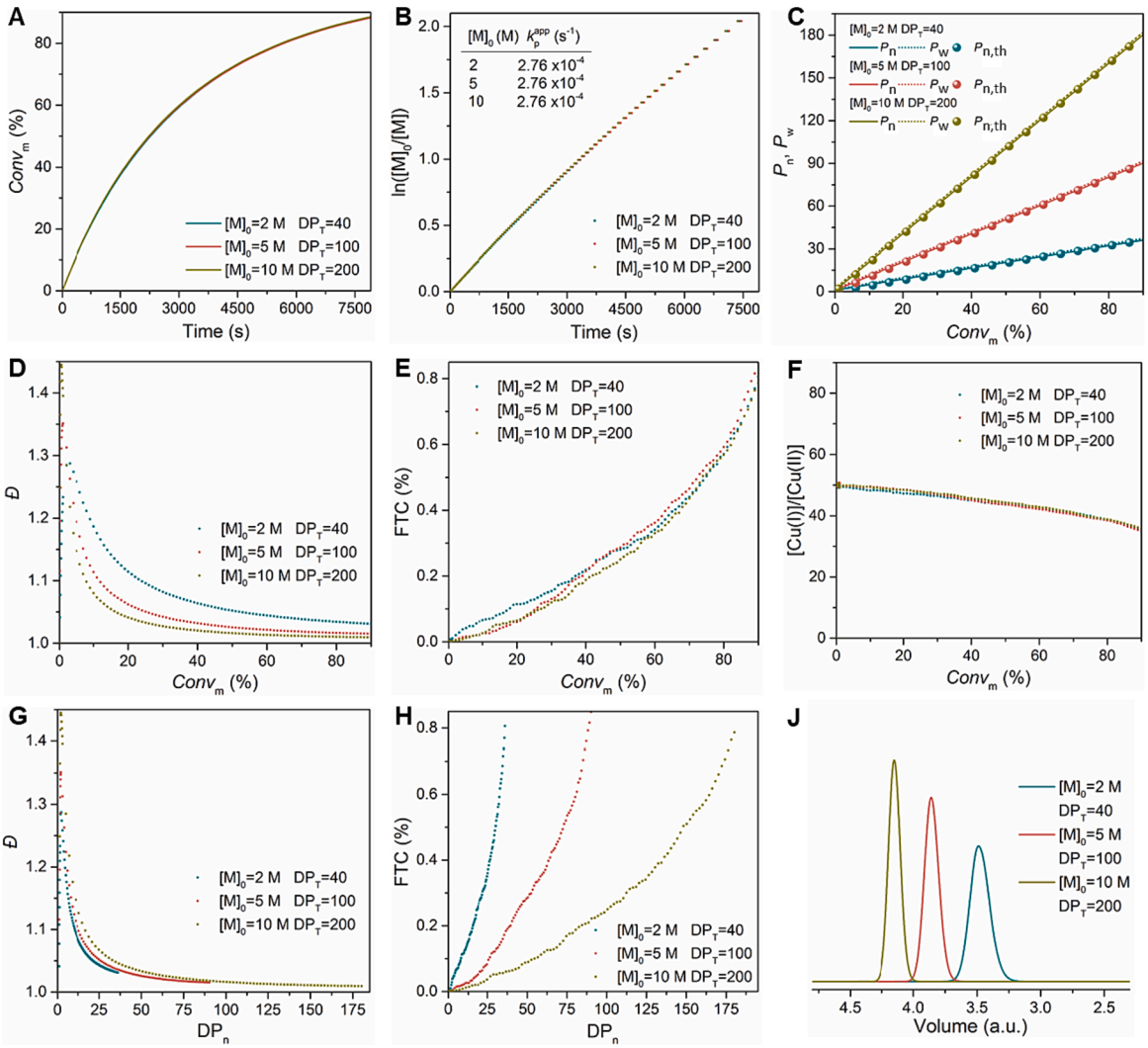

Fig. 3. Monte Carlo simulations of ATRP of MA with different $[M]_0$ and varied DP_T. Kinetic plots of (**A**) $Conv_m$, (**B**) $\ln([M]_0/[M])$ *versus* time (where k_p^{app} is the pseudo-first-order apparent propagation rate constant, i.e., slope of the semilogarithmic kinetic plots). Changes of (**C**) P_n, P_w, (**D**) $Đ$, (**E**) FTC, and (**F**) [Cu(I)]/[Cu(II)] with $Conv_m$. Changes of (**G**) $Đ$, and (**H**) FTC with DP_n. (**J**) MWD at $Conv_m$ = 80%. Results were obtained from Monte Carlo simulations of ATRP of MA at 25 °C with $[M]_0$ = 2 ($[M]_0/[P\text{-}X]_0$ = 40/1), 5 ($[M]_0/[P\text{-}X]_0$ = 100/1), and 10 ($[M]_0/[P\text{-}X]_0$ = 200/1) M, $[P\text{-}X]_0$ = 0.05 M, $[Cu(I)]_0$ = 0.05 M, $[Cu(II)]_0$ = 0.001 M (AKCL increases with increasing $[M]_0$), respectively (Table S3).

obvious with the increase of termination fraction, as shown in Fig. 1.

$$DCF = \frac{DP_T k_t (\ln(1 - Conv_m))^2}{[M]_0 k_p^2 t} \quad (3)$$

where DP_T is the targeted degree of polymerization, defined by the ratio between the initial monomer concentration ($[M]_0$) and the initiator concentration, assuming quantitative initiation (we have removed here the factor 2 present in the original equation by applying the corrected version of the termination equation[29]). $Conv_m$, k_p, k_t, and t are monomer conversion, propagation rate constant, termination rate constant, and time, respectively.

The dead chain fraction (DCF) depends on the set of parameters that can be experimentally adjusted, such as polymerization rate (time, t), monomer conversion and its initial concentration, as well as initiator concentration (or DP_T). The agreement of FTC values predicted by Eqs. (2), 3, and S24 (general FTC) with values obtained by Monte Carlo simulations and the numerical integration of the formulated differential equations (NIDE) is excellent for relatively low FTC.

It is worth noting that both equations have some limitations. Eq. (3) cannot predict DCF for any considered $Conv_m$ if kinetics (e.g. the slope of the semilogarithmic plot, equal approximately to $\ln(1\text{-}Conv_m)/t$) is not known. The practical application of Eq. (2) is also limited in cases where measuring the ratio [Cu(I)]/[Cu(II)] is difficult. Nevertheless, the difference of the new equation from the previous one lies in the ATRP control mechanism it revealed. FTC shows that when termination is negligible, FTC for the given conversion is independent of the $[M]_0$ and $[M]_0/[P\text{-}X]_0$, but depends on the ratio $k_t \times k_{act}[Cu(I)])/(k_p \times k_{de}[Cu(II)])$. Thus, for the specific ATRP system (known k_t and k_p), FTC should depend on the ratio $k_{act}[Cu(I)]/k_{de}[Cu(II)]$. For the given quotient $k_{act}[Cu(I)]/k_{de}[Cu(II)]$ (equal to the proportion of radicals and dormant species), the absolute values of the numerator and denominator determine the dynamics of interconversions of growing radicals and dormant species: the higher are these values, the shorter are periods of growing chains being in the active state.[32-34] Moreover, based on the new FTC formula (Eq. (2)), the livingness and control (dispersity, Eqs. (4) to (6)) in ATRP can be correlated with each other.

As mentioned in the Introduction, though the regulation of dispersity has been discussed many times and various design rules/factors have been employed, a universal design guide has not been demonstrated. In this work, the previous dispersity equation (Eq. (4)),[15] which defined dispersity as the function of $Conv_m$, polymer polymerization degree (DP_n), k_p, k_{de}, [Cu(II)] and the concentration of initiator (dormant

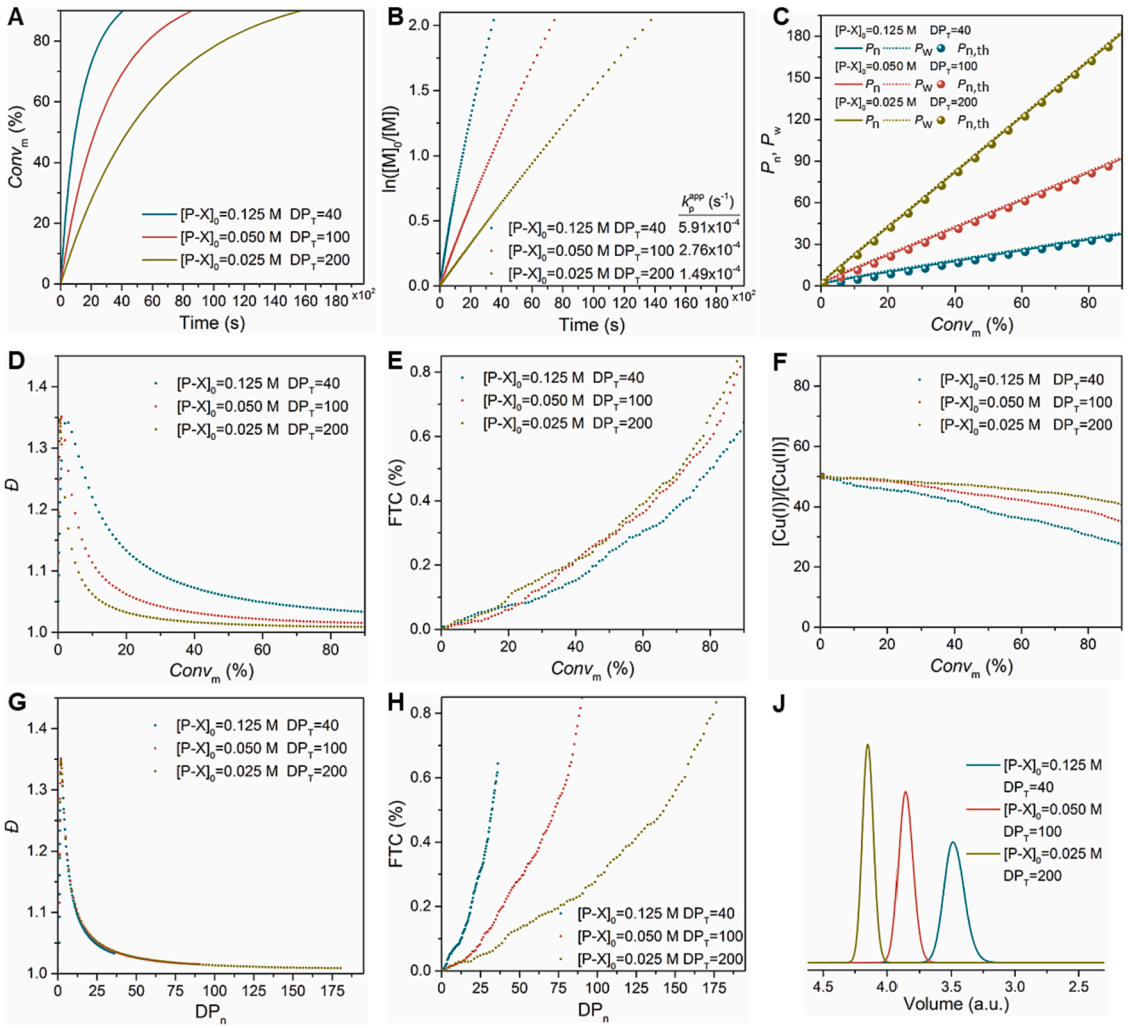

Fig. 4. Monte Carlo simulations of ATRP of MA with different $[P\text{-}X]_0$ and varied DP_T. Kinetic plots of (A) $Conv_m$, (B) $\ln([M]_0/[M])$ *versus* time (where k_p^{app} is the pseudo-first-order apparent propagation rate constant, i.e., slope of the semilogarithmic kinetic plots). Changes of (C) P_n, $P_{w,}$ (D) Đ, (E) FTC, and (F) [Cu(I)]/[Cu(II)] with $Conv_m$. Changes of (G) Đ, and (H) FTC with DP_n. (J) MWD at $Conv_m = 80\%$. Results were obtained from Monte Carlo simulations of ATRP of MA at 25 °C with $[P\text{-}X]_0 = 0.125$ ($[M]_0/[P\text{-}X]_0 = 40/1$, $[R\cdot] = 4.48 \times 10^{-8}$ M), 0.05 ($[M]_0/[P\text{-}X]_0 = 100/1$, $[R\cdot] = 2.09 \times 10^{-8}$ M), and 0.025 ($[M]_0/[P\text{-}X]_0 = 200/1$, $[R\cdot] = 1.13 \times 10^{-8}$ M) M, $[M]_0 = 5$ M, $[Cu(I)]_0 = 0.05$ M, $[Cu(II)]_0 = 0.001$ M (no effect on AKCL), respectively (Table S4). The average $[R\cdot]=k_p^{app}/k_p$, calculated based on the simulated semilogarithmic kinetic plots (Fig. 4B).

species [P-X]), was rearranged to Eq. (5) and (6) to include the new factor of AKCL, thus in synergy with other approaches of this work (simulation, experiment, and mechanism analysis) to demonstrate the effect of AKCL on *Đ*.

$$Đ = 1 + \frac{1}{DP_n} + \left(\frac{k_p[P-X]}{k_{de}[Cu(II)]}\right)\left(\frac{2}{Conv_m} - 1\right) \quad (4)$$

Defining the targeted *DP* as the ratio of initial concentrations of monomer and initiator, $DP_T = [M]_0/[P\text{-}X]_0$, and $Conv_m = DP_n/DP_T$, provided Eq. (5) and Eq. (6). For the given DP_T, the polymer dispersity decreases with decreasing AKCL, and the dispersity is lower with the increase of $Conv_m$ or DP_n. Note that a ratio $AKCL/DP_T$ can be defined as relative AKCL, meaning that dispersity will depend not only on how many monomer units are added at one activation period (actual AKCL) but rather on the number of intermittent activations during the growth of the entire chain.

$$Đ = 1 + \frac{1}{DP_T \times Conv_m} + \frac{AKCL}{DP_T}\left(\frac{2}{Conv_m} - 1\right) \quad (5)$$

$$Đ = 1 + \frac{1}{DP_n} + \frac{AKCL}{DP_T}\left(\frac{2DP_T}{DP_n} - 1\right) \quad (6)$$

2.3. Effect of different parameters on FTC and Đ in ATRP systems

With the monomer fixed (predominately affecting k_p), the effect of the following parameters can be examined in a normal ATRP system: $[M]_0$, $[P\text{-}X]_0$, $Conv_m$, [Cu(I)], [Cu(II)], and k_{de}. By analyzing the above equations of FTC and *Đ*, the effect of changing the initial values of one parameter at a time, in terms of improving or worsening FTC and *Đ* can be clearly seen, as listed in Table 1. However, some of these parameters are related, e.g., $Conv_m = DP_n/DP_T$, $DP_T = [M]_0/[P\text{-}X]_0$, and thus their effects cannot be analyzed independently. Moreover, if termination is extensive, the discussed equations (Eqs. (2) – (6)) would be invalid and conclusions stemming from them could not be drawn. Therefore, to confirm the above analytical results, Monte Carlo simulations[35] were also conducted to evaluate the effect of the above parameters on ATRP control (*Đ* and FTC). The general systems of ATRP of MA were simulated under varying reaction conditions (Table S2 to S9, Fig. 2 to Fig. 7, Fig. S1 and S2; Table S10 to S16, Fig. S3 to S13. See detailed Monte Carlo procedure and parameters in the Supplementary Information).

[M]₀. $[M]_0$ is a parameter that cannot be independently regulated, its variation would either change the concentration of other reagents (by diluting the reaction system with solvent) or varying concurrently DP_T

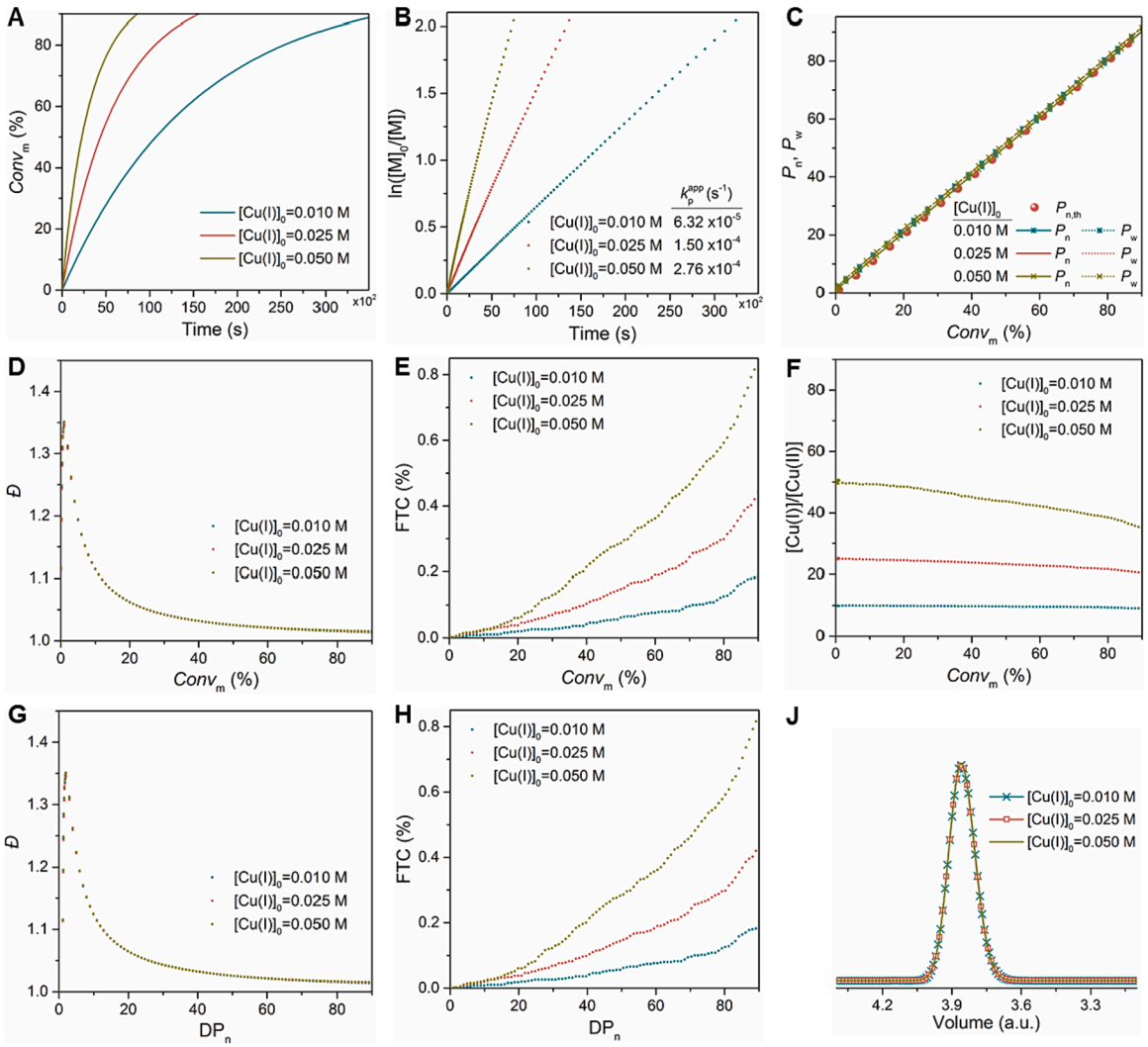

Fig. 5. Monte Carlo simulations of ATRP of MA with different [Cu(I)]. Kinetic plots of (A) $Conv_m$, (B) $\ln([M]_0/[M])$ *versus* time (where k_p^{app} is the pseudo-first-order apparent propagation rate constant, i.e., slope of the semilogarithmic kinetic plots). Changes of (C) P_n, P_w, (D) Đ, (E) FTC, and (F) [Cu(I)]/[Cu(II)] with $Conv_m$. Changes of (G) Đ, and (H) FTC with DP_n. (J) MWD at $Conv_m$ = 80%. Results were obtained from Monte Carlo simulations of ATRP of MA at 25 ℃ with $[Cu(I)]_0$ = 0.01 ($[R\cdot] = 4.79 \times 10^{-9}$ M), 0.025 ($[R\cdot] = 1.14 \times 10^{-8}$ M), and 0.05 ($[R\cdot] = 2.09 \times 10^{-8}$ M) M, $[M]_0$ = 5 M, $[P\text{-}X]_0$ = 0.05 M, $[Cu(II)]_0$ = 0.001 M (no effect on AKCL), respectively (Table S6). $[M]_0/[P\text{-}X]_0$ = 100/1. Average $[R\cdot]=k_p^{app}/k_p$, calculated based on the simulated semilogarithmic kinetic plots (Fig. 5B).

(by keeping all concentrations constant except $[M]_0$, meaning changing $[M]_0/[P\text{-}X]_{0\ M}$ ratio). Herein, both cases were simulated to evaluate the effect of varied $[M]_0$ on FTC and Đ. Fig. 2 shows the simulation results with $[M]_0$ of 10, 5, and 2 M respectively by diluting the system while keeping DP_T constant (i.e., 100). In this case, for a higher value of $[M]_0$, neither the polymer dispersity (Đ and MWD, Fig. 2D and 2 J) nor the fraction of terminated chains (FTC, Fig. 2E) was affected, where only a faster polymerization rate was observed (Fig. 2A and 2B). The above conclusions are also applicable for the effect of other parameters ($[P\text{-}X]_0$, $[Cu(I)]_0$, and $[Cu(II)]_0$), the concentration of which were also changed by dilution, while no effect on FTC and Đ was observed. The same conclusions can also be drawn from the analytical equations (Eqs. (2) to (6)), however, due to the advantageous of Monte Carlo simulations, [36,37] more characteristics in real experiments can be seen from the simulated results, such as the influence of accumulated terminations on the reduction of the [Cu(I)]/[Cu(II)] ratios (Fig. 2F).

Fig. 3 displays the simulation results by keeping all other concentrations constant and only changing the $[M]_0$ (with a value of 10, 5, and 2 M respectively). Therefore, as shown in Fig. 3C, at the same $Conv_m$, DP_n obtained from three systems varied. Similar to the above case, different $[M]_0$ did not affect FTC (Fig. 3E), however, there is a decrease of Đ in the system with higher $[M]_0$, which was caused by the higher DP_n, due to the statistical broadening item in Eqs. (4) to (6) becoming more negligible when DP increased. However, if we compare the influence on FTC and Đ in respect to DP_n, the observed effect is different. At the same DP_n, Đ is higher with the increase of $[M]_0$ (Fig. 3G), while FTC is lower (Fig. 3H). This is due to the lower $Conv_m$ in the system with higher $[M]_0$ for the same DP_n (Eqs. (2) – (5)).

[P-X]₀. By varying only $[P\text{-}X]_0$ while keeping all other reagent concentrations constant, DP_T was varied concurrently. Under this condition, according to Fig. 4B, a higher value of $[P\text{-}X]_0$ caused the increased radical concentration ($[R\cdot]=k_p^{app}/k_p$). However, the increase degree of $[R\cdot]$ is much lower than that of $[P\text{-}X]_0$, resulting in the ratio of [Cu(I)]/[Cu(II)] decreasing with conversion (Fig. 4F). Therefore, according to the FTC equation (Eq. (3)), a lower FTC should be obtained with the higher $[P\text{-}X]_0$. This is confirmed by the simulation results in Fig. 4E (this effect is more obvious in the simulations with lower initial [Cu(II)], Fig. S5 and S6). Regarding Đ, it changed in an opposite way to FTC, i.e., at a given $Conv_m$, Đ increased with the higher value of $[P\text{-}X]_0$ (Fig. 4D), which can also be concluded according to the dispersity equations (increased DP_T and DP_n in Eqs. (4) – (6)). However, due to the varied DP_T in these systems, the observed effect on FTC and Đ is opposite

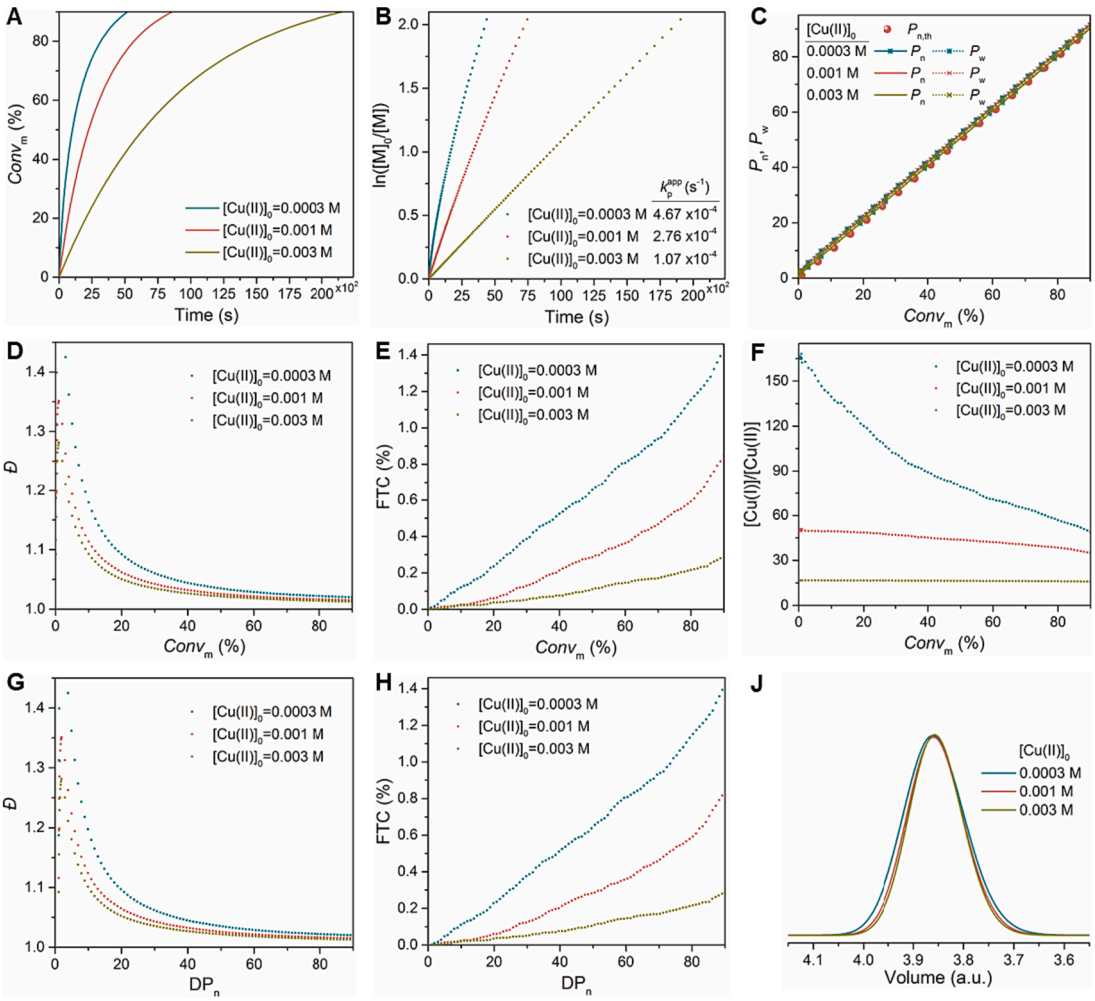

Fig. 6. Monte Carlo simulations of ATRP of MA with different [Cu(II)]. Kinetic plots of (A) $Conv_m$, (B) ln([M]$_0$/[M]) *versus* time (where k_p^{app} is the pseudo-first-order apparent propagation rate constant, i.e., slope of the semilogarithmic kinetic plots). Changes of (C) P_n, P_w, (D) Đ, (E) FTC, and (F) [Cu(I)]/[Cu(II)] with $Conv_m$. Changes of (G) Đ, and (H) FTC with DP_n. (J) MWD at $Conv_m$ = 80%. Results were obtained from Monte Carlo simulations of ATRP of MA at 25 ℃ with [Cu(II)]$_0$ = 0.0003 ([R·] = 3.54 × 10^{-8} M), 0.001 ([R·] = 2.09 × 10^{-8} M), and 0.003 ([R·] = 8.11 × 10^{-9} M) M, [M]$_0$ = 5 M, [P-X]$_0$ = 0.05 M, [Cu(I)]$_0$ = 0.05 M (AKCL decreases with increasing [Cu(II)]$_0$), respectively (Table S7). [M]$_0$/[P-X]$_0$ = 100/1. Average [R·]=k_p^{app}/k_p, calculated from the semilogarithmic kinetic plots (Fig. 6B).

when comparing at the same DP_n. As shown in Fig. 4G and 4H, Đ slightly decreased with the increase of [P-X]$_0$ at the same DP_n, while FTC increased, due to the higher $Conv_m$ in the system with higher [P-X]$_0$ for the same DP_n (Eqs. (2) – (5)). DP_T stayed constant if changing both [P-X]$_0$ and [M]$_0$, while keeping their ratios constant (Table S5 and S13). Under this case, Đ should increase with the increase of [P-X]$_0$ and [M]$_0$ (Eqs. (4) – (6)), and FTC should decrease due to the decreased ratio of [Cu(I)] and [Cu(II)] (Eq. (3)). This is confirmed by the simulation results in Fig. S1 and Fig. S11.

Conv$_m$. The effect of $Conv_m$ on Đ and FTC is illustrated by Monte Carlo simulations (Figs. 2 – 4) and according to the equations of Đ and FTC (Eqs. (2) – (6)). As listed in Table 1, in certain systems, the higher the $Conv_m$, the lower the Đ, however, the higher the FTC.

[Cu(I)]. Monte Carlo simulations of ATRP of MA were conducted with three different [Cu(I)]$_0$ (0.01, 0.025, and 0.05 M) to investigate the influence of [Cu(I)] on Đ and FTC. According to Fig. 5B, the increased value of [Cu(I)]$_0$ caused the increased k_p^{app}, i.e., the increased average [R·] (k_p^{app}/k_p) and a shorter reaction time (t). Therefore, as can be observed in Fig. 5E, more terminations happened in the system with higher [Cu(I)]$_0$, which is also consistent with the predictions – higher DCF (Eq. (2)) or FTC (Eq. (3)) should be obtained with the lower value of t or the higher ratio of [Cu(I)]/[Cu(II)] (Fig. 5F). [Cu(I)] is an irrelevant factor with Đ cf. Eqs. (4) – (6) and the results of the simulation (Fig. 5D).

Nevertheless, thanks to the advantages of Monte Carlo simulations in revealing more realistic changes in a polymerization compared to the analytical equations,[36,37] it can be noted that in ATRP systems with a lower initial value of [Cu(II)]$_0$ (Table S14), polymer dispersity can be slightly improved due to higher [Cu(II)] generated by the higher [Cu(I)]$_0$ (Fig. S7 and S8).

[Cu(II)]. To reflect the effect of changing [Cu(II)] on FTC and Đ, Monte Carlo simulations were performed by keeping all initial parameters constant, except for setting [Cu(II)]$_0$ as 0.0003, 0.001 and 0.003 M respectively. Fig. 6D and Fig. 6E show that with a higher concentration of deactivator [Cu(II)]$_0$, both the values of Đ and FTC were lower. The same conclusion is also drawn by analyzing the DCF/FTC and Đ equations (Eqs. (2) – (6)).This indicates that increase of [Cu(II)]$_0$ is beneficial for both a decrease of Đ and a decrease of FTC.

k_{de}. In an ATRP system, k_{de} can be adjusted by using various solvent, ligand, and catalyst (though this adjustment is less flexible as compared to [Cu(II)], as it needs to match with the monomer activity and solubility. The values of k_{de} under different ATRP conditions are accessible from Ref. [15] and [38] according to the ligands, initiators and solvents). Similar to the influence of [Cu(II)], the effect of increasing k_{de} on narrowing the MWD and suppressing the radical terminations was proved by the lower Đ and FTC obtained in Fig. 7D and Fig. 7E *via* the Monte Carlo simulations. However, if changing both k_{de} and k_{act}, while

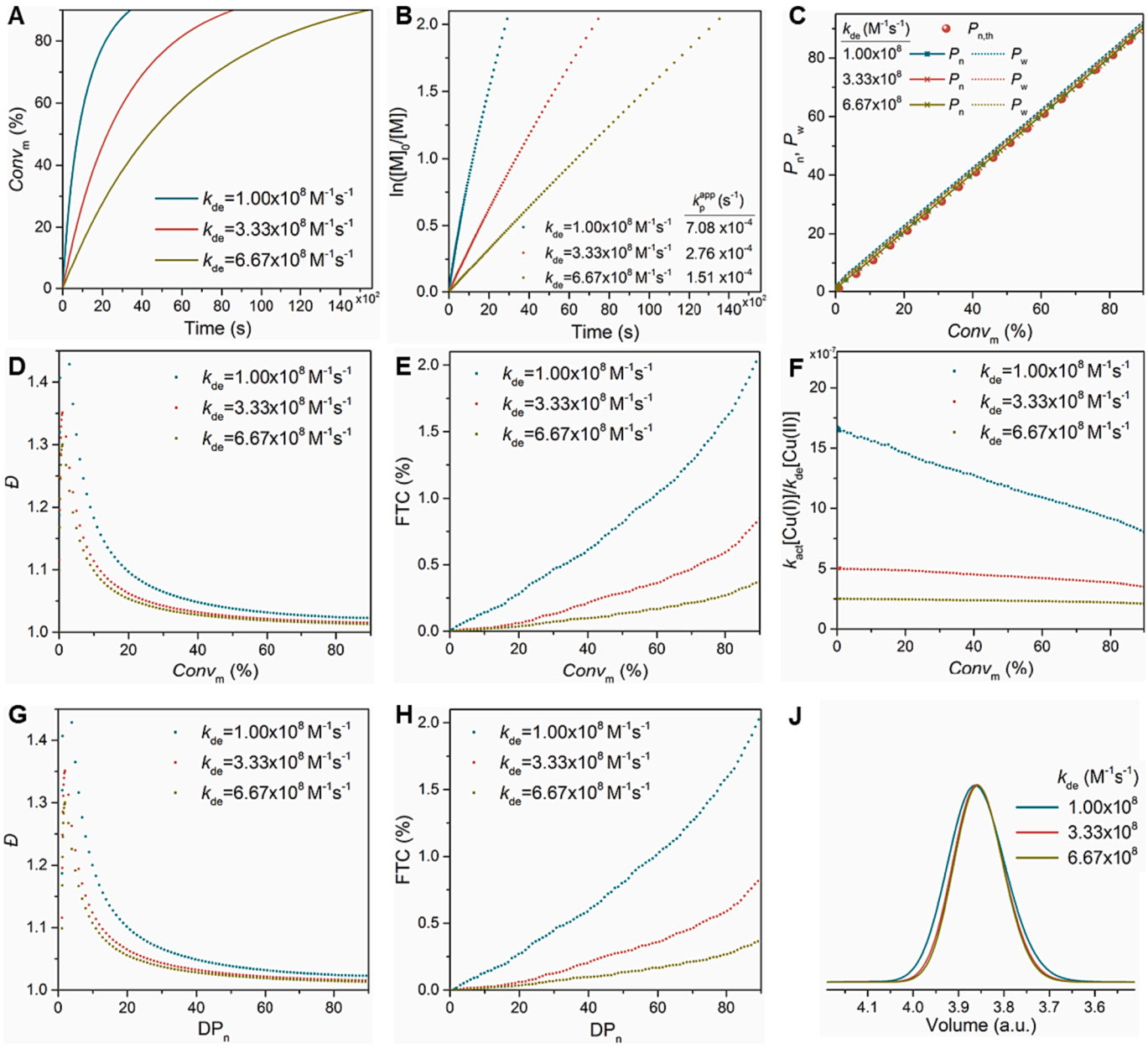

Fig. 7. Monte Carlo simulations of ATRP of MA with different k_{de}. Kinetic plots of (A) $Conv_m$, (B) $\ln([M]_0/[M])$ *versus* time (where k_p^{app} is the pseudo-first-order apparent propagation rate constant, i.e., slope of the semilogarithmic kinetic plots). Changes of (C) P_n, P_w, (D) Đ, (E) FTC, and (F) $k_{act}[Cu(I)]/k_{de}[Cu(II)]$ with $Conv_m$. Changes of (G) Đ, and (H) FTC with DP_n. (J) MWD at $Conv_m$ = 80%. Results were obtained from Monte Carlo simulations of ATRP of MA at 25 °C with k_{de} = 1×10^8 ($[R\cdot] = 5.36 \times 10^{-8}$ M), 3.33×10^8 ($[R\cdot] = 2.09 \times 10^{-8}$ M), and 6.67×10^8 ($[R\cdot] = 1.14 \times 10^{-8}$ M) M^{-1} s^{-1}, $[M]_0$ = 5 M, $[P\text{-}X]_0$ = 0.05 M, $[Cu(II)]_0$ = 0.05 M, $[Cu(II)]_0$ = 0.001 M (AKCL decreases with increasing k_{de}) respectively (Table S8). $[M]_0/[P\text{-}X]_0$ = 100/1. Average $[R\cdot]=k_p^{app}/k_p$, calculated based on the simulated semilogarithmic kinetic plots (Fig. 7B).

keeping the ratio of k_{act}/k_{de} constant, only Đ was affected, and FTC stayed constant (Table S9, Fig. S2). This is achieved by changing the activation/deactivation dynamics while keeping the same ratio of $k_{act}[Cu(I)]/k_{de}[Cu(II)]$ (Eq. (3)).[32-34].

2.4. The illustration of AKCL for ATRP control

The above analysis results demonstrate that among various parameters affecting ATRP ($[M]_0$, $[P\text{-}X]_0$, $Conv_m$, [Cu(I)], [Cu(II)], and k_{de}), [Cu(II)] and k_{de} are two parameters that can simultaneously diminish both Đ and FTC (Table 1). As introduced at the beginning of this paper, targeting a particular ATRP system with specific k_p and $[M]_0$, the effect of [Cu(II)] and k_{de} can be represented by one unique concept – AKCL, the larger k_{de} and/or the higher concentration of deactivator ([Cu(II)]), the smaller the AKCL, and the lower Đ and FTC. This regulation mechanism is illustrated in Fig. 8.

For very small AKCL achieved by increasing the value of [Cu(II)] or k_{de} (top box, Fig. 8), as described by the FTC equation (Eq. (2)), the importance of small AKCL for controlling ATRP FTC stems from adjusting the ratio of concentrations of active chains to dormant chains. The small AKCL increases the ratio of $k_{de}[Cu(II)]/k_{act}[Cu(I)]$ and leads to a smaller fraction of active chains, thus suppressing the terminations. In ATRP growing chains change intermittently from dormant to active form. When AKCL is small (top box, Fig. 8), polymer chains change many times from dormant (deactivated) to active state. As a result, only a small number of monomeric units can be added to the growing chain

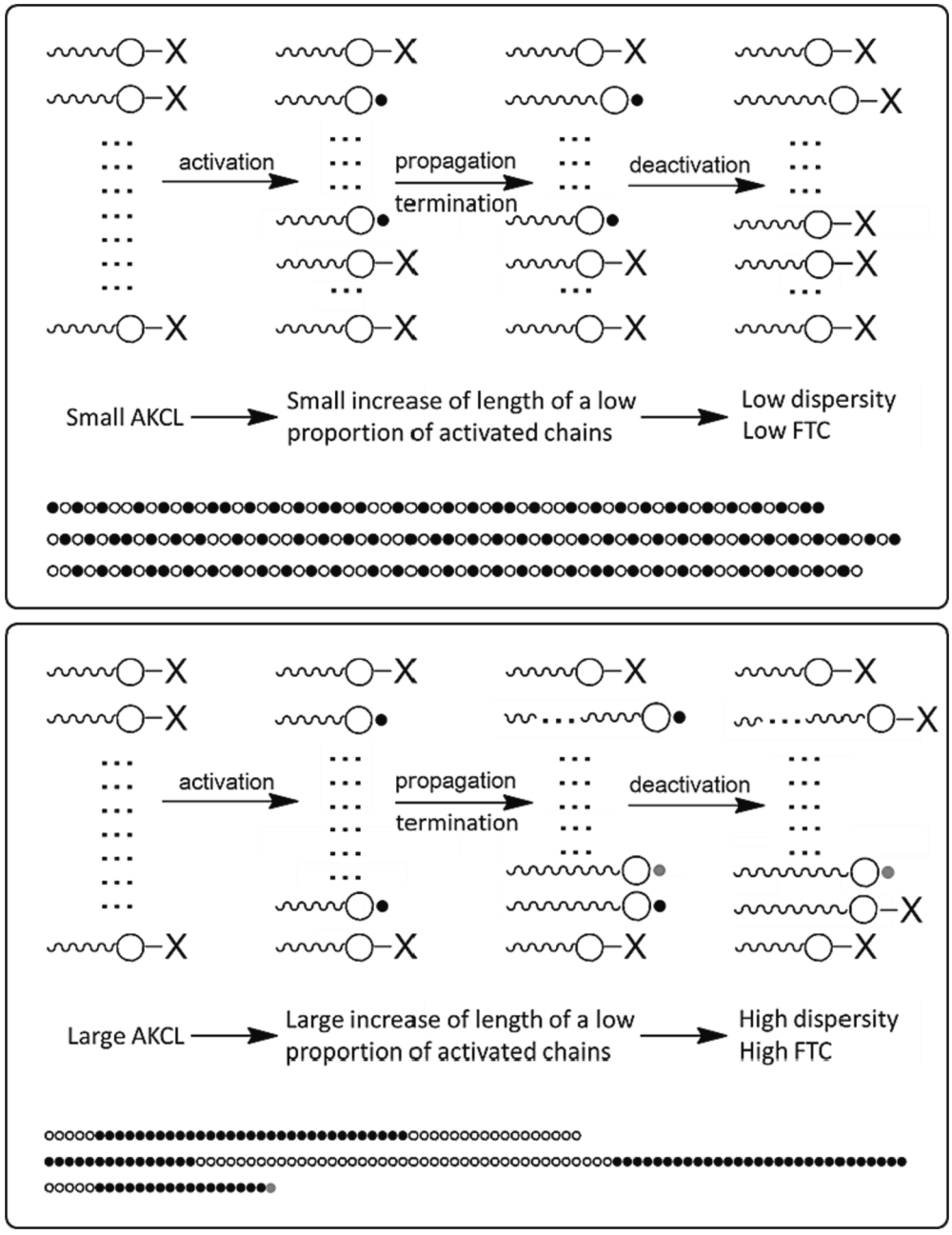

Fig. 8. Schematic illustration of the control mechanism of AKCL in ATRP. Differences in formation of polymer in the well-designed ATRP system (low AKCL, top box) and the poorly controlled ATRP system (large AKCL, bottom box) with the same targeted DP. Schematic presentation of polymer chains with white and black monomeric units reflects number of monomeric units attached in different time intervals of a chain being activated (sets of units alternately marked with different colors), the grey monomeric unit represent the terminated chain end.

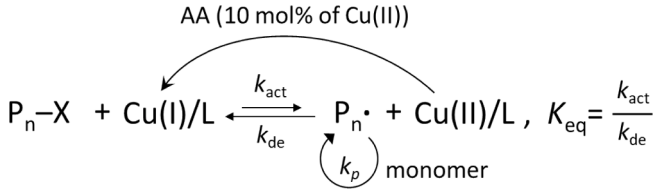

Scheme 2. Schematic illustration of the mechanism of DE-ATRP. Deactivation enhanced strategy is achieved by adding a low amount of reducing agent (typically, 10 mol% of Cu(II)).[40,41] AA is the ascorbic acid. K_{eq} is the ATRP equilibrium constant.

ends. This mode of chain growth leads to concurrent growth of all chains. Therefore, dispersity of polymer is low and MWD resembles the Poisson distribution. On the other hand, when AKCL is large (bottom box, Fig. 8), in the active state a large number of monomers are added. The distribution of numbers of attached units is geometric, resulting in broader distribution of polymer chains and higher dispersity. Also, the larger AKCL due to a lower value of [Cu(II)] or k_{de} (bottom box, Fig. 8), decreases the ratio of k_{de}[Cu(II)]/k_{act}[Cu(I)] and leads to a larger portion of active chains, thus enhancing the terminations, as described by the FTC equation (Eq. (2)).

2.5. Application of small AKCL in experimental design

To verify the effect of AKCL in ATRP, experiments that follow the small AKCL design principle were conducted (it should be noted that in experiements, k_p at low $Conv_m$ is much higher, by about one order of magnitude above average k_p,[39] this variance should be taken into account when ultilizing the small AKCL criterion so as to avoid undesired control at the very early stage). Deactivation-enhanced ATRP (DE-ATRP)[40,41] is a typical example using increased [Cu(II)] to achieve smaller AKCL for a better control. As illustrated in Scheme 2, DE-ATRP, similar to the AGET (activators generated by electron transfer) ATRP,

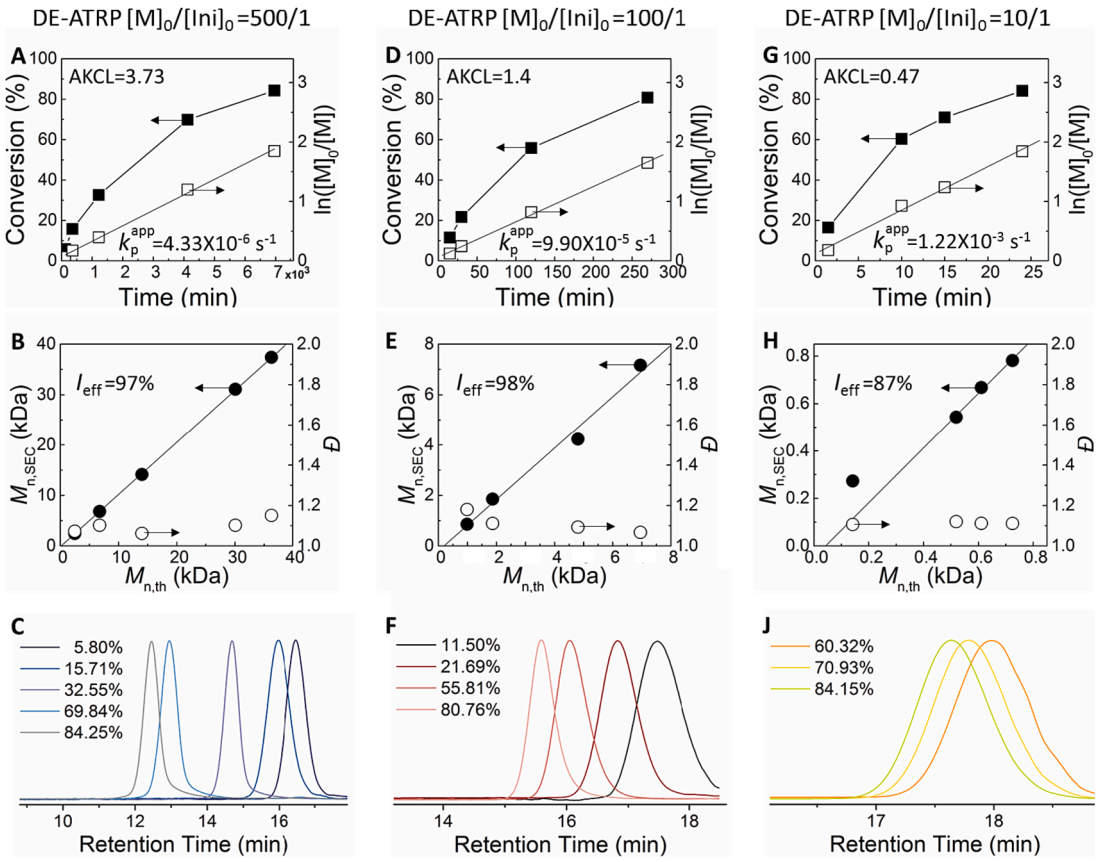

Fig. 9. Well-controlled polymerization of DE-ATRP of MA with different $[M]_0/[Ini]_0$ under small AKCL control. Kinetic plots of $Conv_m$ and $\ln([M]_0/[M])$ *versus* time (**A**, **D**, and **G,** where k_p^{app} is the pseudo-first-order apparent propagation rate constant, i.e., the slope of the semilogarithmic kinetic plots, average $[R\cdot]=k_p^{app}/k_p$ (Table S17)), plots of $M_{n,SEC}$ and $Đ$ *versus* $M_{n,th}$ (**B**, **E**, and **H**, the slope in the plots of $M_{n,SEC}$ *versus* $M_{n,th}$ represents the initiator efficiency - I_{eff}), and the evolution of MW monitored by SEC (**C**, **F**, and **J**) with $[M]_0/[Ini]_0 = 500/1$ (**A**, **B**, and **C,** AKCL = 3.73, $[R\cdot] = 1.55 \times 10^{-10}$ M), 100/1 (**D**, **E**, and **F,** AKCL = 1.4, $[R\cdot] = 3.54 \times 10^{-9}$ M), 10/1 (**G**, **H**, and **J,** AKCL = 0.47, $[R\cdot] = 4.36 \times 10^{-8}$ M), Results were obtained from DE-ATRP of MA with $[M]_0/[Ini]_0/[Cu(II)]_0/[AA]_0/[L]_0 = 500/1/0.625/0.125/0.625$, 100/1/0.25/0.025/0.25 and 100/10/0.75/0.075/0.75, tris[2-(dimethylamino)ethyl]amine (Me_6TREN) as a ligand in butanone at 70 ℃ (Table 2).

Table 2
^{1}H NMR and SEC analysis of DE-ATRP of MA[a].

	$[M]_0/[Ini]_0$	$[M]_0$ (M)	Time (min)	AKCL[b]	$M_{n,th}^c$ (kDa)	$M_{n,SEC}^d$ (kDa)	$Đ^d$	$Conv_m^e$ (%)
1	500/1	5.00	120	3.73	2.50	2.46	1.07	5.8
2			360		6.76	6.83	1.10	15.7
3			1220		14.0	14.1	1.06	32.6
4			4125		30.1	31.1	1.10	69.8
5			6960		36.3	37.4	1.15	84.3
6	100/1	5.00	15	1.4	0.99	0.86	1.18	11.5
7			30		1.87	1.85	1.11	21.7
8			120		4.81	4.23	1.09	55.8
9			270		6.95	7.17	1.07	80.8
10	10/1	5.00	1.5	0.47	0.14	0.27	1.11	16.5
11			10		0.52	0.54	1.12	60.3
12			15		0.61	0.67	1.11	70.9
13			24		0.72	0.78	1.11	84.2

[42] uses a reducing agent (e.g., ascorbic acid, AA) to reduce the copper-based catalyst from the higher oxidation state to the lower (active) state for the activation of alkyl halide initiators, hence leading to the radical formation and chain propagation. However, DE-ATRP differs from other recent ATRP procedures based on the continuous regeneration of activators, such as ARGET (activators regenerated by electron transfer) ATRP,[43] SARA (supplemental activator and reducing agent) ATRP, [44] ICAR (initiators for continuous activator regeneration),[45] photoATRP (photochemically induced ATRP),[46,47] mechanoATRP (mechanically controlled ATRP)[48] or eATRP (electrochemically mediated ATRP)[49]. Compared to the high amount of reducing agent used for other ATRP procedures (e.g., 10-fold $Sn(EH)_2$ *vs* Cu(II) in ARGET ATRP, over 10-fold AIBN *vs* Cu(II) in ICAR ATRP, excess zerovalent metals in SARA ATRP etc), the important difference is that DE-ATRP uses low proportions of reducing agent (typically, 10 mol% of AA *vs* Cu(II)) added at the beginning of the reaction to retain a large proportion of the Cu complex in the higher oxidation state, Cu(II) (note that 1 AA reduces 2 Cu(II) species) (Scheme 2). The selection of such a low level of reducing agent *vs* Cu(II) in DE-ATRP makes its AKCL value extreme small, thus benefial for the control.

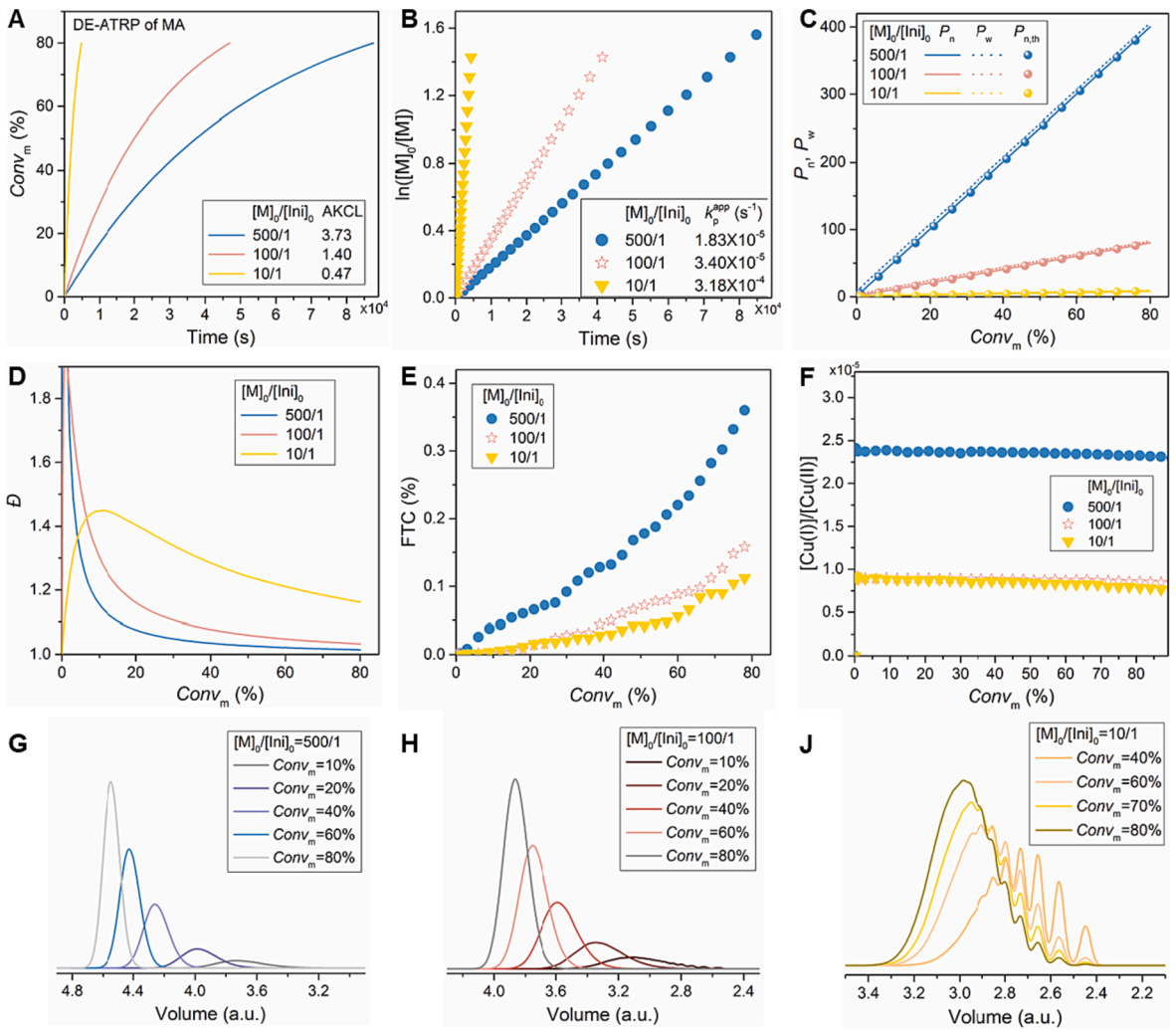

Fig. 10. Monte Carlo simulation of the well-controlled polymerization of DE-ATRP of MA with different $[M]_0/[Ini]_0$. Kinetic plots of (**A**) $Conv_m$, (**B**) $\ln([M]_0/[M])$ *versus* time (where k_p^{app} is the pseudo-first-order apparent propagation rate constant, i.e., slope of the semilogarithmic kinetic plots). Changes of (**C**) P_n, P_w, (**D**) $Đ$, (**E**) FTC, and (**F**) [Cu(I)]/[Cu(II)] with $Conv_m$. (**G**) (**H**) (**J**) MWD at $Conv_m = 80\%$. Results were obtained from the simulations of DE-ATRP of MA at 70 °C with $[M]_0/[Ini]_0$–500/1 (AKCL = 3.73, $[R\cdot] = 6.53 \times 10^{-10}$ M), 100/1 (AKCL = 1.4, $[R\cdot] = 1.21 \times 10^{-9}$ M), and 10/1 (AKCL = 0.47, $[R\cdot] = 1.14 \times 10^{-8}$ M), $[M]_0 = 5$ M, $[Ini]_0 =$ 0.01, 0.05, and 0.5 M, $[Cu(I)]_0 = 0.0025$, 0.0025, 0.0075 M, $[Cu(II)]_0 = 0.0038$, 0.01, 0.03 M, respectively (Table S17). Average $[R\cdot]=k_p^{app}/k_p$ (Table S17).

Herein, DE-ATRPs of MA with different ratios of initial concentrations of monomer and initiator ($[M]_0/[Ini]_0 = 500/1$, 100/1, and 10/1 respectively) were experimentally studied. The AKCL in each system was calculated based on Eq. (1). As depicted in Fig. 9A, Fig. 9D and Fig. 9G, under the control of small AKCL, in all cases, straight semilogarithmic kinetic plots indicated insignificant termination. In general, good agreement between the SEC measured number-averaged MW ($M_{n,SEC}$) and the theoretical number-averaged MW ($M_{n,th}$) were observed, especially for lower $[Ini]_0$ (Fig. 9B, Fig. 9E and Fig. 9H, Table 2). Polymers with low dispersity ($Đ$~1.10) and with progressively shifted SEC traces with no tailings were obtained (Fig. 9C, Fig. 9F and Fig. 9J). The application of the small AKCL criterion also contributed to the suppression of secondary reactions of acrylate monomers (which are subject to backbiting even at low temperatures (<80 °C)[50]) *via* the significant enhanced competitive deactivation reactions of radicals, thus achieved better control.

a) DE-ATRP of MA: $[M]_0/[Ini]_0/[Cu(II)]_0/[AA]_0/[L]_0 = 500/1/0.625/0.125/0.625$, 100/1/0.25/0.025/0.25 and 100/10/0.75/0.075/0.75, M = MA, Ini = EBriB, Cu(II) = $CuBr_2$, AA = L-ascorbic acid, L = Me_6TREN, Solvent = Butanone, T = 70 °C, b) AKCL was calculated based on Eq. (1), c) $M_{n,th} = ([M]_0/[Ini]_0) \times$ Monomer conversion ($Conv_m$) × MW(M), d) $M_{n,SEC}$ and $Đ$ were determined in relation to poly-MA standards using SEC equipped with a RI detector, e) $Conv_m$ was determined by ^{1}H NMR.

Then, Monte Carlo simulation were employed here to simulate the DE-ATRP of MA under the same reaction conditions ($[M]_0/[Ini]_0 = 500/1$, 100/1, 10/1, Table S17, detailed model and algorithm description is provided in the Supporting Information). The simulation results are displayed in Fig. 10. They are consistent with the experimental data, for small AKCL, well-controlled DE-ATRPs were obtained, reflected by the linear and steady chain propagations with narrow MWDs, low $Đ$ (Fig. 10D), leading to < 0.40% terminated chains (FTC, Fig. 10E).

Lower $Đ$ were obtained for higher targeted DP since the absolute values of $Đ$ not only depend on the AKCL but also DP_T and DP_n, as defined by Eq. (5). Specifically, as the results shown in Table 2 and Fig. 10, though the AKCL of 500/1 system is almost 8 times bigger than that of 10/1 system, the DP_T of 500/1 is 50 times bigger than 10/1, thus the absolute values of $Đ$ in 500/1 system is still lower than the 10/1 system. Therefore, with a predetermined DP_T, the general design guideline is that a smaller AKCL is more beneficial for control without the need to compromise the DP_T. Under this criterion, the universal selection strategy of AKCL for good control in different conditions would be $k_t[R\cdot] \ll k_p[M] \ll k_{de}[Cu(II)]$. However, this control could be too much for some high DP systems, thus with the above relationship, the AKCL

values could be further adjusted based on the specific *DP*s and requirements on $Đ$ (Eq. (5)) and FTC (Eq. (2)).

Conversely, in each of these systems, increasing the values of AKCL decreased control (i.e., higher dispersity and higher FTC). For example, in Monte Carlo simulation for DE-ATRP of MA with $[M]_0/[Ini]_0 = 100/1$, the increased ratio of $[AA]_0$ to $[Cu(II)]_0$ from to 10 to 20, 30, 40%, decreased the ratio [Cu(II)]/Cu(I)] from 0.2/0.05 to 0.15/0.1 to 0.1/0.15 and to 0.05/0.2 and correspondingly increased the AKCL by 1.3, 2, and 4 times respectively (Table S18). As shown in Fig. S14 – S16, compared to the previously shown well-controlled DE-ATRP system (AKCL = 1.4), diminished control in these systems with larger AKCL was clearly observed, which is illustrated by the broader MWD and higher $Đ$. Moreover, under the same DP_T, the lower AKCLs led to slower polymerization rates, reflected from the lower values of slopes of $Conv_m$ *vs*. *t* traces in Fig. S16. The FTC increased from 0.1 to 1%, which agrees with the derived equation for FTC (Eq. (2)): for the increased ratio of k_{act}[Cu(I)]/k_{de}[Cu(II)]. Under established ATRP equilibrium, this ratio is also equal to [R·]/[P-X]. Consequently, FTC increased for higher [R·], i.e., faster polymerization (and even faster termination) and for longer targeted chains (lower [P-X]). Interestingly, FTC should not change if the reaction rate would increase to the same degree as [P-X] (i.e., keeping k_{act}[Cu(I)]/k_{de}[Cu(II)] constant), as illustrated in the above cases of changing targeted *DP* from 10 to 100. The absolute concentration of terminated chains for $DP_T = 10$ is 10 times higher than for $DP_T = 100$ system, a similar FTC was observed due to the similar k_{act}[Cu(I)]/k_{de}[Cu(II)] in these two systems (Fig. 10F). However, if changing targeted *DP* from 100 (or 10) to 500, the ratio of [Cu(I)]/[Cu(II)] (or [R·]/[P-X]) increased due to the use of a higher ratio of AA (20 mol % *vs* $[Cu(II)]_0$, Table 2, Table S17), leading to a higher FTC.

3. Conclusions

In terms of the various parameters that affect the ATRP process and product structure, this work for the first time demonstrated what the most benefical factor is for ATRP control by systematically examining the effect of each individual parameter on livingness and dispersity *via* the combination of analytical equations, Monte Carlo simulations, and wet experiments. It was shown that the low AKCL value can be used as a general guidline for achieving a well-controlled ATRP process. Targeting a particular ATRP system (with set values of k_p, $[M]_0$, and $[M]_0/[Ini]_0$), smaller AKCL can simultaneously suppress chain terminations (FTC) and decrease dispersity of polymer chains. This universal criterion is easy to follow during the experimental design, and the implementation of which does not compromise the predetermined DP_T and reaction concentration etc. It is expected that this AKCL criterion could also be extended to other controlled/living polymerization systems, which will be studied in our future work.

Declaration of Competing Interest

The authors declare that they have no known competing financial interests or personal relationships that could have appeared to influence the work reported in this paper.

Data availability

Data will be made available on request.

Acknowledgments

We thank the Irish Research Council (IRC) Government of Ireland Postdoctoral Fellowship (GOIPD/2022/209), Science Foundation Ireland (SFI) Frontiers for the Future 2019 call (19/FFP/6522), the statutory funds of Centre of Molecular and Macromolecular Studies, Polish Academy of Sciences, and NSF (CHE 2000391) for funding this research.

Appendix A. Supplementary data

Supplementary data to this article can be found online at https://doi.org/10.1016/j.cej.2023.145548.

References

[1] PlasticsEurope. *Plastics – the Facts 2020*; 2020.
[2] P. Nesvadba, Radical Polymerization in Industry. Encyclopedia of Radicals in Chemistry, Biology and Materials, John Wiley & Sons Ltd:, Chichester, UK, 2012.
[3] K. Matyjaszewski, T.P. Davis (Eds.), Handbook of Radical Polymerization, Wiley, 2002.
[4] C. Walling, Free Radicals in Solution, John Wiley & Sons Inc, 1957.
[5] C.H. Bamford, The Kinetics of Vinyl Polymerization by Radical Mechanisms, Academic Press, 1958.
[6] G. Moad, D.H. Solomon, The Chemistry of Radical Polymerization, Elsevier, 2006.
[7] A.D. Jenkins, R.G. Jones, G. Moad, Terminology for Reversible-Deactivation Radical Polymerization Previously Called "Controlled" Radical or "Living" Radical Polymerization (IUPAC Recommendations 2010), Pure Appl. Chem. 82 (2) (2010) 483–491.
[8] C.M. Fellows, R.G. Jones, D.J. Keddie, C.K. Luscombe, J.B. Matson, K. Matyjaszewski, J. Merna, G. Moad, T. Nakano, S. Penczek, G.T. Russell, P. D. Topham, Terminology for chain polymerization (IUPAC Recommendations 2021), Pure Appl. Chem. 94 (9) (2022) 1093–1147.
[9] N. Corrigan, K. Jung, G. Moad, C.J. Hawker, K. Matyjaszewski, C. Boyer, Reversible-Deactivation Radical Polymerization (Controlled/Living Radical Polymerization): From Discovery to Materials Design and Applications, Prog. Polym. Sci. 111 (2020), 101311.
[10] K. Matyjaszewski, J. Xia, Atom Transfer Radical Polymerization, Chem. Rev. 101 (2001) 2921–2990.
[11] J. Wang, K. Matyjaszewski, Controlled/"Living" Radical Polymerization. Atom Transfer Radical Polymerization in the Presence of Transition-Metal Complexes, J. Am. Chem. Soc. 117 (1995) 5614–5615.
[12] F. Lorandi, M. Fantin, K. Matyjaszewski, Atom Transfer Radical Polymerization: A Mechanistic Perspective, J. Am. Chem. Soc. 144 (34) (2022) 15413–15430.
[13] Chiefari, J.; Chong, Y. K. (Bill); Ercole, F.; Krstina, J.; Jeffery, J.; Le, T. P. T.; Mayadunne, R. T. A.; Meijs, G. F.; Moad, C. L.; Moad, G.; Rizzardo, E.; Thang, S. H. Living Free-Radical Polymerization by Reversible Addition-Fragmentation Chain Transfer: The RAFT Process. *Macromolecules* **1998**, *31*, 5559–5562.
[14] M.K. Georges, R.P.N. Veregin, P.M. Kazmaier, G.K. Hamer, Narrow Molecular Weight Resins by a Free-Radical Polymerization Process, Macromolecules 26 (11) (1993) 2987–2988.
[15] K. Matyjaszewski, Atom Transfer Radical Polymerization (ATRP): Current Status and Future Perspectives, Macromolecules 45 (10) (2012) 4015–4039.
[16] K. Matyjaszewski, Advanced Materials by Atom Transfer Radical Polymerization, Adv. Mater. 30 (23) (2018) 1706441.
[17] K. Matyjaszewski, N.V. Tsarevsky, Macromolecular Engineering by Atom Transfer Radical Polymerization, J. Am. Chem. Soc. 136 (2014) 6513–6533.
[18] R. Yin, Z. Wang, M.R. Bockstaller, K. Matyjaszewski, Tuning Dispersity of Linear Polymers and Polymeric Brushes Grown from Nanoparticles by Atom Transfer Radical Polymerization, Polym. Chem. 12 (42) (2021) 6071–6082.
[19] R. Whitfield, K. Parkatzidis, M. Rolland, N.P. Truong, A. Anastasaki, Tuning Dispersity by Photoinduced Atom Transfer Radical Polymerisation: Monomodal Distributions with Ppm Copper Concentration, Angew. Chemie - Int. Ed. 58 (38) (2019) 13323–13328.
[20] R. Whitfield, N.P. Truong, D. Messmer, K. Parkatzidis, M. Rolland, A. Anastasaki, Tailoring Polymer Dispersity and Shape of Molecular Weight Distributions: Methods and Applications, Chem. Sci. 10 (38) (2019) 8724–8734.
[21] D.T. Gentekos, R.J. Sifri, B.P. Fors, Controlling Polymer Properties through the Shape of the Molecular-Weight Distribution, Nat. Rev. Mater. 4 (12) (2019) 761–774.
[22] M.-N. Antonopoulou, R. Whitfield, N.P. Truong, A. Anastasaki, Controlling Polymer Dispersity Using Switchable RAFT Agents: Unravelling the Effect of the Organic Content and Degree of Polymerization, Eur. Polym. J. 174 (2022), 111326.
[23] Miao, Y.-P.; Lyu, J.; Yong, H.-Y.; A, S.; Gao, Y.-S.; Wang, W.-X. Controlled Polymerization of Methyl Methacrylate and Styrene via Cu(0)-Mediated RDRP by Selecting the Optimal Reaction Conditions. *Chinese J. Polym. Sci.* **2019**, *37* (6), 591–597.
[24] D. Wang, X. Li, W.-J. Wang, X. Gong, B.-G. Li, S. Zhu, Kinetics and Modeling of Semi-Batch RAFT Copolymerization with Hyperbranching, Macromolecules 45 (1) (2012) 28–38.
[25] G. Litvinenko, A.H.E. Müller, General Kinetic Analysis and Comparison of Molecular Weight Distributions for Various Mechanisms of Activity Exchange in Living Polymerizations, Macromolecules 30 (96) (1997) 1253–1266.
[26] A.H.E. Müller, G. Litvinenko, D. Yan, Kinetic Analysis of "Living" Polymerization Systems Exhibiting Slow Equilibria. 4. "Dissociative" Mechanism of Group Transfer Polymerization and Generation of Free Ions in Cationic Polymerization, Macromolecules 29 (7) (1996) 2346–2353.
[27] S. Penczek, G. Moad, Glossary of Terms Related to Kinetics, Thermodynamics, and Mechanisms of Polymerization, Pure Appl. Chem. 80 (2008) 2163–2193.
[28] W. Tang, K. Matyjaszewski, Kinetic Modeling of Normal ATRP, Normal ATRP with [CuII]0, Reverse ATRP and SR&NI ATRP, Macromol. Theory Simulations 17 (7–8) (2008) 359–375.

[29] R. Szymanski, On the Incorrectness of the Factor 2 in the Radical Termination Equation, Macromol. Theory Simulations 20 (1) (2011) 8–12.
[30] R. Szymanski, On the Possibility of Different Reactivity of Growing Radicals in Controlled and Free Radical Polymerizations. The Concept of the Reaction Cage in Controlled Radical Polymerization, Macromol. Theory Simulations 30 (2) (2021) 2000078.
[31] M. Zhong, K. Matyjaszewski, How Fast Can a CRP Be Conducted with Preserved Chain End Functionality? Macromolecules 44 (8) (2011) 2668–2677.
[32] W. Tang, Y. Kwak, W.A. Braunecker, N.V. Tsarevsky, M.L. Coote, K. Matyjaszewski, Understanding Atom Transfer Radical Polymerization: Effect of Ligand and Initiator Structures on the Equilibrium Constants, J. Am. Chem. Soc. 130 (32) (2008) 10702–10713.
[33] R. Szymanski, S. Sosnowski, Cumulative Steady State Monte Carlo Method for Processes with Exchange between Reactive Species. Case of Controlled Radical Copolymerization, Chem. Eng. J. 370 (2019) 432–443.
[34] S. Sosnowski, R. Szymanski, A Novel Efficient Hybrid Algorithm for Monte Carlo Simulation of Controlled Radical Polymerization: The Method Integrating Reactive and Deactivated Species, Chem. Eng. J. 358 (2019) 197–210.
[35] R.Y. Rubinstein, D.P. Kroese, Simulation and the Monte Carlo Method, 3rd Ed, John Wiley & Sons, 2017.
[36] Figueira, F. L.; Trigilio, A. D.; Wu, Y. Y.; Zhou, Y. N.; Luo, Z. H.; Van Steenberge, P. H. M.; D'hooge, D. R. Explicit Stochastic Modeling of Termination Chain Length Dependencies for All Disparate Radical Pairs in Single Phase Free Radical Induced Grafting. *Chem. Eng. J.* **2023**, *452*, 139389.
[37] Marien, Y. W.; Edeleva, M.; Figueira, F. L.; Arraez, F. J.; Van Steenberge, P. H. M.; D'hooge, D. R. Translating Simulated Chain Length and Molar Mass Distributions in Chain-Growth Polymerization for Experimental Comparison and Mechanistic Insight. *Macromol. Theory Simulations* **2021**, *30*, 2100008.
[38] M. Horn, K. Matyjaszewski, Solvent Effects on the Activation Rate Constant in Atom Transfer Radical Polymerization, Macromolecules 46 (9) (2013) 3350–3357.
[39] A.A. Gridnev, S.D. Ittel, Dependence of Free-Radical Propagation Rate Constants on the Degree of Polymerization, Macromolecules 29 (18) (1996) 5864–5874.
[40] W. Wang, Y. Zheng, E. Roberts, C.J. Duxbury, L. Ding, D.J. Irvine, S.M. Howdle, Controlling Chain Growth: A New Strategy to Hyperbranched Materials, Macromolecules 40 (20) (2007) 7184–7194.
[41] Y. Zheng, H.L. Cao, B. Newland, Y.X. Dong, A. Pandit, W. Wang, 3D Single Cyclized Polymer Chain Structure from Controlled Polymerization of Multi-Vinyl Monomers: Beyond Flory-Stockmayer Theory, J. Am. Chem. Soc. 133 (33) (2011) 13130–13137.
[42] W. Jakubowski, K. Matyjaszewski, Activator Generated by Electron Transfer for Atom Transfer Radical Polymerization, Macromolecules 38 (10) (2005) 4139–4146.
[43] W. Jakubowski, K. Min, K. Matyjaszewski, Activators Regenerated by Electron Transfer for Atom Transfer Radical Polymerization of Styrene, Macromolecules 39 (1) (2006) 39–45.
[44] D. Konkolewicz, Y. Wang, M. Zhong, P. Krys, A.A. Isse, A. Gennaro, K. Matyjaszewski, Reversible-Deactivation Radical Polymerization in the Presence of Metallic Copper. A Critical Assessment of the SARA ATRP and SET-LRP Mechanisms, Macromolecules 46 (22) (2013) 8749–8772.
[45] K. Matyjaszewski, W. Jakubowski, K. Min, W. Tang, J. Huang, W.A. Braunecker, N. V. Tsarevsky, Diminishing Catalyst Concentration in Atom Transfer Radical Polymerization with Reducing Agents, Proc. Natl. Acad. Sci. U. S. A. 103 (42) (2006) 15309–15314.
[46] D. Konkolewicz, K. Schroder, J. Buback, S. Bernhard, K. Matyjaszewski, Visible Light and Sunlight Photoinduced ATRP with Ppm of Cu Catalyst, ACS Macro Lett. 1 (2012) 1219–1223.
[47] G. Szczepaniak, J. Jeong, K. Kapil, S. Dadashi-Silab, S.S. Yerneni, P. Ratajczyk, S. Lathwal, D.J. Schild, S.R. Das, K. Matyjaszewski, Open-Air Green-Light-Driven ATRP Enabled by Dual Photoredox/Copper Catalysis, Chem. Sci. 13 (39) (2022) 11540–11550.
[48] Z. Wang, X. Pan, J. Yan, S. Dadashi-Silab, G. Xie, J. Zhang, Z. Wang, H. Xia, K. Matyjaszewski, Temporal Control in Mechanically Controlled Atom Transfer Radical Polymerization Using Low Ppm of Cu Catalyst, ACS Macro Lett. 6 (5) (2017) 546–549.
[49] P. Chmielarz, M. Fantin, S. Park, A.A. Isse, A. Gennaro, A.J.D. Magenau, A. Sobkowiak, K. Matyjaszewski, Electrochemically Mediated Atom Transfer Radical Polymerization (EATRP), Prog. Polym. Sci. 69 (2017) 47–78.
[50] T. Pirman, M. Ocepek, B. Likozar, Radical Polymerization of Acrylates, Methacrylates, and Styrene: Biobased Approaches, Mechanism, Kinetics, Secondary Reactions, and Modeling, Ind. Eng. Chem. Res. 60 (26) (2021) 9347–9367.